Journal of Neuroimmunology 208 (2009) 136–140

Contents lists available at ScienceDirect

Journal of Neuroimmunology

journal homepage: www.elsevier.com/locate/jneuroim

Short communication

CD8 positive T-cell infiltration in the dentate nucleus of paraneoplastic cerebellar degeneration

Moe Moe Aye [a], Takefumi Kasai [a], Yukie Tashiro [b], Hui Qin Xing [a], Hiroshi Shirahama [b], Minoru Mitsuda [c], Takayuki Suetsugu [b], Keiko Tanaka [d], Mitsuhiro Osame [e], Shuji Izumo [a,*]

[a] Molecular Pathology, Center for Chronic Viral Diseases, Kagoshima University Graduate School of Medical and Dental Sciences, Kagoshima, Japan
[b] Imakiire General Hospital, Kagoshima, Japan
[c] Okatsu Hospital, Kagoshima, Japan
[d] Department of Neurology, Brain Research Institute, Niigata University, Niigata, Japan
[e] Department of Neurology and Geriatrics, Kagoshima University Graduate School of Medical and Dental Sciences, Kagoshima, Japan

ARTICLE INFO

Article history:
Received 5 August 2008
Received in revised form 8 January 2009
Accepted 12 January 2009

Keywords:
Paraneoplastic cerebellar degeneration
Dentate nucleus
T-cell infiltration
Autopsy

ABSTRACT

Recent reports have discussed the presence of cytotoxic T cells in paraneoplastic cerebellar degeneration (PCD). We report an autopsy case of PCD associated with anti-Hu antibody, in which we revealed infiltration of CD8+ T cells in and around the dentate nucleus but not in the cerebellar cortex, in addition to severe Purkinje cell loss. Some infiltrated mononuclear cells expressed cytotoxic cell marker, Granzyme B. Decrease of neurons and reduced presynapses were demonstrated in the dentate nucleus. This is the first report that suggests the possibility of the dentate nucleus being primarily attacked followed by Purkinje cell loss in PCD.

1. Introduction

Paraneoplastic cerebellar degeneration (PCD) is a disease associated with cancer, particularly small cell lung cancer (SCLC), gynecological cancers and Hodgkin's disease. Clinical and pathological features of PCD are rapid progressive development of pancerebellar dysfunction and diffuse loss of Purkinje cells respectively (Posner, 1993). Autoantibodies, for example anti-Yo and anti-Ri for gynaecological and breast cancer and anti-Hu for lung cancer, are considered to play a role in the pathogenesis of PCD (Anderson et al., 1988; Furneaux et al., 1990; Shams'ili et al., 2003). In the late 1990s, some reports have postulated that T cells play a role in pathogenesis of PCD (Albert et al., 1998; Tanaka et al., 1999). However, there are very few reports about T cell or mononuclear cell infiltrations in the cerebellar lesions of PCD.

This is the first report that shows infiltrations of CD8+ T cells in the dentate nucleus in the absence of similar infiltration in the cerebellar cortex and an apparent decrease of dentate neurons, in addition to degeneration of cerebellar cortex in PCD.

2. Materials and methods

2.1. Case report

A 70-year-old man was admitted with developing cerebellar ataxia and dysarthria in December 2003. Magnetic Resonance Imaging of brain revealed no abnormalities. Two days later, consciousness disturbance occurred and the increased mononuclear cells (104/mm^3), mainly lymphocytes (95%), and increased protein content (64 mg/dl) in cerebrospinal fluid were found. With a diagnosis of possible viral encephalitis, he was treated with intravenous Acyclovir; however, the symptoms progressed. Two courses of intravenous IgG were given because an immune-mediated disorder like brain stem encephalitis was suspected, and consciousness was recovered. However, cerebellar ataxia was not improved. After 6 months, the patient developed superior vena cava syndrome due to a mediastinal tumor. The patient received oncotherapy with Cisplatin and Topotecan, 70 mg/body each, for lung cancer, but after two weeks of starting oncotherapy, he died of bronchopneumonia.

The autopsy showed a small cell carcinoma of the right lung as a primary tumor and combined small cell /giant cell carcinoma in the mediastinal tumor as a metastasis. Serum anti-Hu antibody was positive while anti-Yo, anti-Ri were negative.

* Corresponding author. Tel.: +81 992 75 5940; fax: +81 992 75 5942.
E-mail address: izumo@m.kufm.kagoshima-u.ac.jp (S. Izumo).

0165-5728/$ – see front matter © 2009 Elsevier B.V. All rights reserved.
doi:10.1016/j.jneuroim.2009.01.017

2.2. Histopathological examination

In addition to routine histological examination, we performed immunohistochemistry using mouse monoclonal antibodies (mAbs) anti-CD3, anti-CD4 (1: 100 Chemicon International), anti-CD8, anti-synaptophysin (1:1000, Chemicon. International), anti-human macrophage CD68 (KP1; 1:50 DAKO), and Granzyme B (1:200, Serotec. UK) with Envision system (DAKO) and biotinylated goat anti-human IgG Ab (1:400, Vector) with Avidin Biotin Complex method on paraffin sections of brain and lung tissues. Immunoreactivity was visualized using diaminobenzidine/peroxidase and Amino-ethylcarbazole substrate-chromogen appropriately. Light counterstaining was done with hematoxylin. Corresponding brain sections from a patient with Duchenne muscular dystrophy were used as a control.

2.3. Scoring of numbers of dentate neurons

The numbers of dentate neurons were counted in one full microscopic field (×100 magnification) from five randomly selected areas of the dentate nucleus. The average number from these five samples was compared to similarly prepared and analyzed dentate nucleus from a Duchenne muscular dystrophy patient used as a control. Statistical analysis was performed using Mann–Whitney's test.

3. Results

The brain weighed 1300 g after fixation. Pathological findings revealed marked and diffuse loss of Purkinje cells and increased Bergmann's glia in the cerebellar hemisphere (Fig. 1a). The cerebellar vermis showed moderate Purkinje cell loss with scattered torpedo formation in granular cell layer (Fig. 1b, c). Many empty baskets and torpedoes were detected with Bodian staining (Fig. 1d, e).

Apparent myelin loss and diffusely distributed foamy macrophages were demonstrated in the amiculum of dentate nucleus (Fig. 2a), and perivascular and parenchymal infiltration of mononuclear cells was noted in and around the dentate nucleus. Dentate neurons appeared smaller than normal, and the number of neurons was decreased (Fig. 2b), the average of which is 44 (SD±4.6) and that of control is 78 (SD±12) with P value<0.001.

By immunohistochemistry, anti-synaptophysin Ab demonstrated apparent decrease of presynapses with enlarged dot-like distribution in and around the dentate neurons (Fig. 2c), whereas in the normal dentate nucleus, diffuse staining of neuropils along with dendritic trees was observed (Fig. 2d). IgG deposition was detected in the cytoplasm of dentate neurons (Fig. 3a). In the cerebellar cortex, a few Golgi cells with IgG deposition were observed in the granular layer, whereas no IgG deposition was detected in any of the remaining Purkinje cells. (Fig. 3b).

Most of the infiltrating mononuclear cells in the dentate were CD3+ and CD8+ T-cells and CD68+ foamy macrophages, particularly at the perivascular area and also closely around the dentate neurons (Fig. 4a, b, c). Some of them expressed Granzyme B, which is a marker of cytotoxic T cells and NK cells (Fig. 4d, e). Only a few perivascular CD8+ T cells were seen in the thalamus, lateral geniculate body, midbrain, pons and the cerebellar white matter; however, none were observed in the cerebellar cortex. In the small cell lung carcinoma, we could

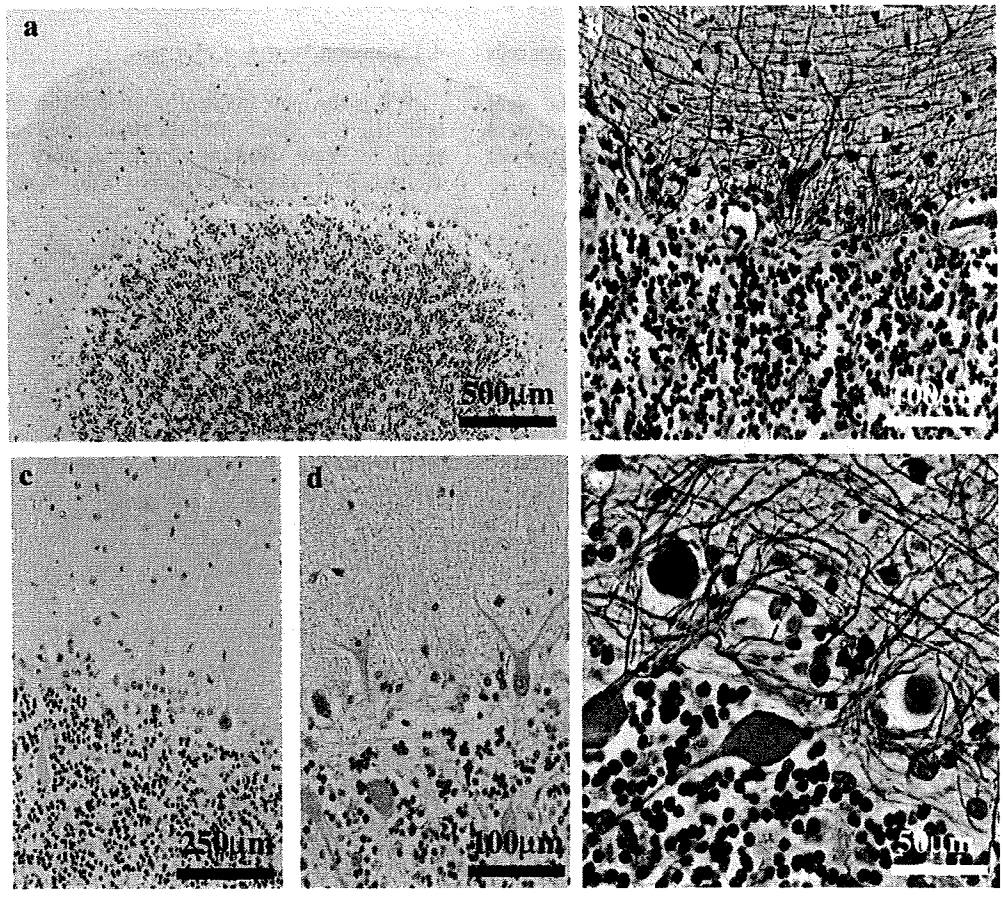

Fig. 1. Cerebellar cortex of the patient stained with HE (a, c, d) and Bodian staining (b, e). Marked and diffuse loss of Purkinje cells (a) and increased Bergmann's glia (c) with empty baskets (b) in the cerebellar hemisphere. Moderate Purkinje cell loss with scattered torpedo formation in the cerebellar vermis (d, e).

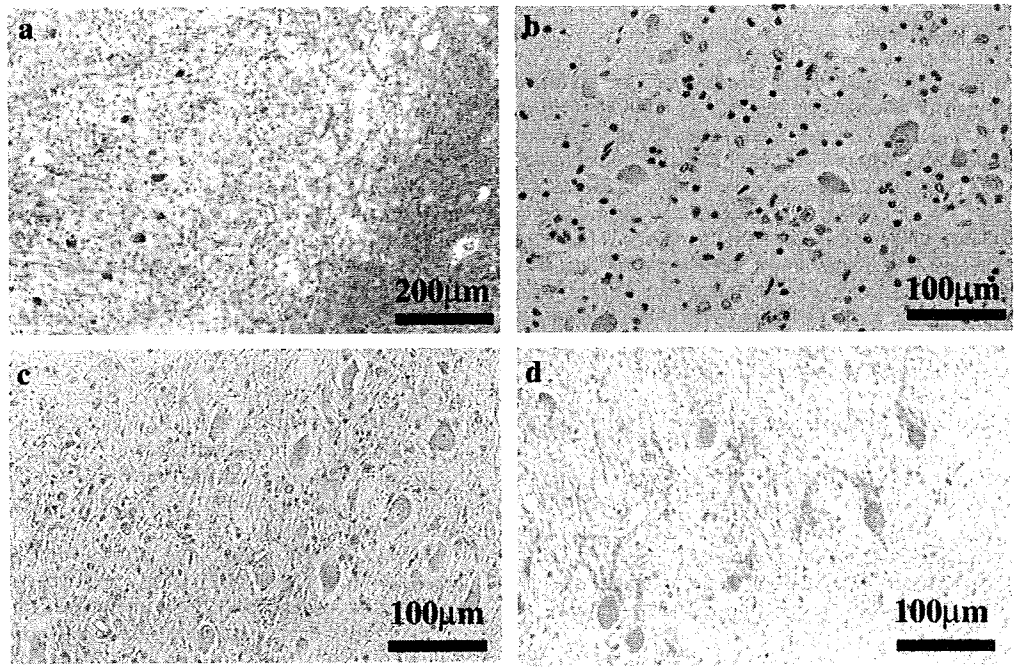

Fig. 2. Dentate nucleus of the patient stained with KB (a), HE (b) and anti-synaptophysin (c), and normal dentate nucleus of Duchenne muscular dystrophy stained with anti-synaptophysin (d). Apparent myelin loss and diffuse foamy macrophages in the amiculum of the dentate nucleus (a). Decrease of dentate neurons with astrocytic gliosis and infiltration of mononuclear cells (b). Apparent decrease of presynapses with dot-like distribution in and around the dentate neurons in PCD (c). Normal dentate showing diffusely stained pattern along with dendritic trees of neurons (d).

detect many invading CD8+ T cells, closely adhering to the tumor cells (Fig. 4f).

A single microscopic, old infarct was detected in the right hippocampus. No other histopathological abnormalities were detected in the entire cerebral cortex, neither in the spinal cord nor in the dorsal root ganglia.

4. Discussion

PCD is the most frequent paraneoplastic syndrome affecting the brain (Liu et al., 2000). Anti-Hu Ab-positive paraneoplastic syndrome tends to show widespread inflammatory infiltrates commonly designated as encephalomyelitis (Graus et al., 2001; Sillevis Smitt

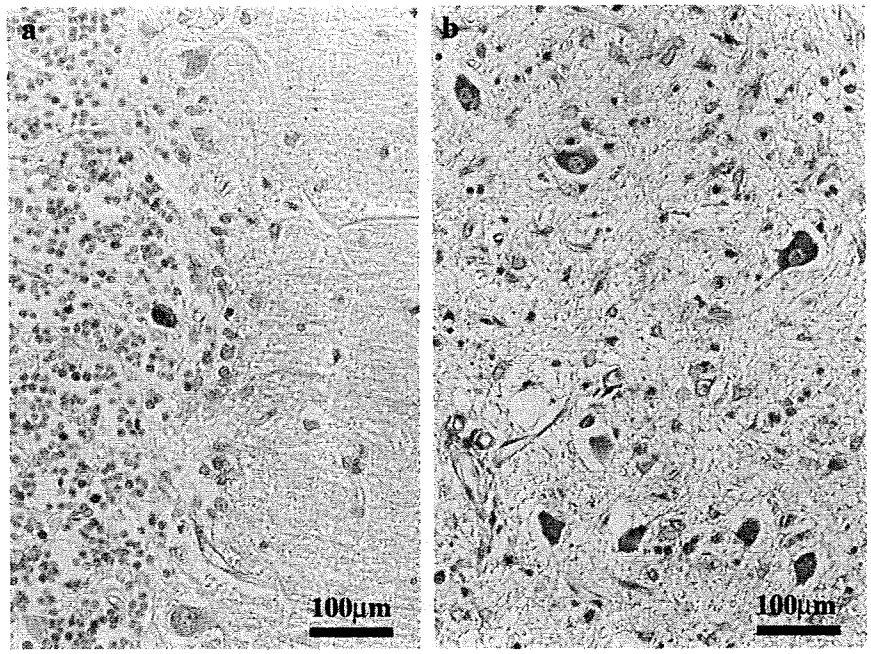

Fig. 3. Cerebellar vermis (a) and dentate neucleus of the patient (b) stained with anti-human IgG Ab. No IgG deposition in the Purkinje cells but in the Golgi cell of cerebellar vermis (a). IgG deposition in the cytoplasm of dentate neurons (b).

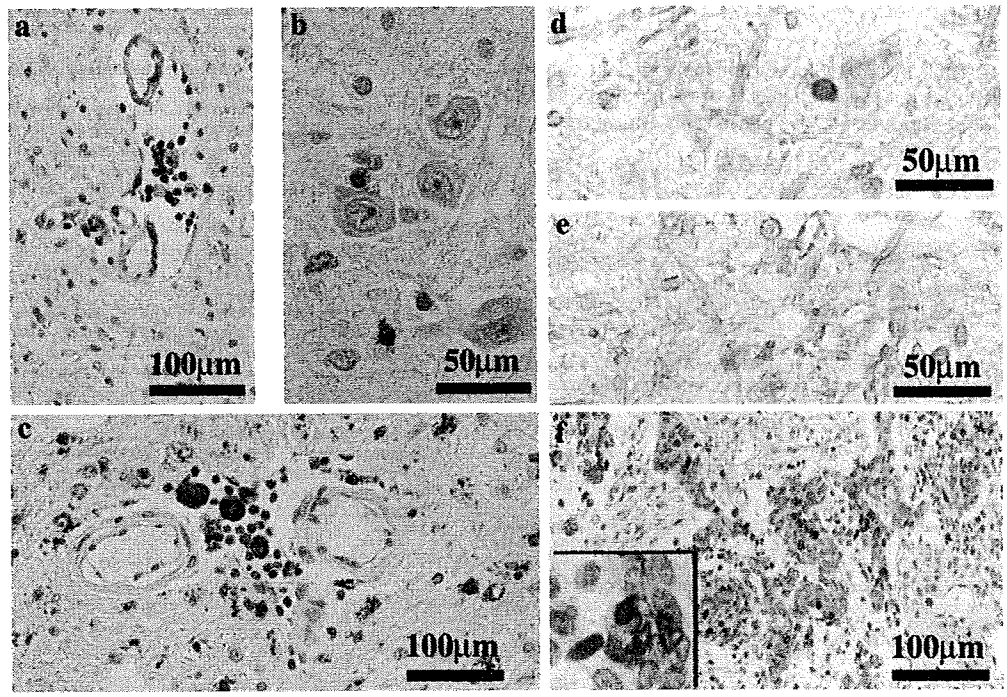

Fig. 4. Immunohistochemistry of infiltrating mononuclear cells in the dentate nucleus stained with antibodies to CD8 (a, b), CD68 (c), Granzyme B (d, e) and in the tumor tissue with CD8 (f). CD8+ infiltrating T-cells present in the perivascular area as well as close to the neurons (a, b). Diffuse and perivascular infiltration of macrophages in and around the dentate nucleus (c) Expression of Granzyme B in mononuclear cell infiltrates close to dentate neurons (d, e). Many CD8+ T cells invading the small cell carcinoma (f) and closely adhering to the tumor cells (inset).

et al., 2002) and subacute sensory neuropathy (Darnell and DeAngelis, 1993). Here, we demonstrated characteristic pathological features of PCD with SCLC as a primary tumor. Although loss of consciousness at the beginning of the disease suggests a possibility of paraneoplastic encephalomyelitis in the present case, pure cerebellar ataxia seen in the late stage of the clinical course and the observation of very few mononuclear cells infiltrating the brain other than the cerebellum were compatible with a pure PCD.

Previous studies focused mainly on auto-antibodies as the effectors of Purkinje cell degeneration in PCD (Greenlee et al., 1993; Darnell and DeAngelis, 1993; Giometto et al., 1997). However, a pathogenic role of these auto-antibodies in causing Purkinje cell loss is not yet known (Rosenblum, 1993). On the other hand, circulating antigen-specific CD8+ T cells are likely to be the effectors of PCD tumor immunity (Albert et al., 1998; Tanaka et al., 1999). In this study, we observed perivascular and parenchymal infiltration of CD8+ T cells in the dentate, but not in the cerebellar cortex. Several reports described inflammatory infiltrates in the PCD, however, most of those cases were encephalomyelitis and inflammatory infiltrates are not restricted in the deep cerebellar nuclei (Henson and Urich, 1982; Verschuuren et al., 1996; Giometto et al., 1997; Brieva-Ruiz et al., 2008). One autopsy case without tumor showed high anti-Ri titers, severe Purkinje cell loss and inflammatory infiltrates involving the brain stem (Hormigo et al., 1994). Therefore, this is the first report of CD8+ T cell infiltration only in the dentate nucleus of the cerebellum, but not in the cerebellar cortex in PCD. Absence of inflammatory infiltrate in the cerebellar cortex in PCD might be explained by a final burn-out stage of inflammation as suggested by Verschuuren et al., 1996. However, in our case, we assume that the cerebellar vermis has not yet reached burn-out, because we could still detect some Purkinje cells preserved and torpedoes. In such a condition of active degeneration, we could not detect any inflammatory infiltrates in the cerebellar vermis but we could detect T-cell infiltration and expression of Granzyme B in the infiltrated T cells close to the neurons in the dentate.

The mechanism of Purkinje cell loss in our PCD case is still uncertain. Although one report demonstrated that anti-Hu Ab may cause destruction of cerebellar neurons in vitro (Greenlee et al., 1993), we did not detect IgG deposition in the remaining Purkinje cells. Instead, we detected IgG deposition in many dentate neurons suggesting that prolonged immune attack on dentate nucleus might cause retrograde degeneration of Purkinje cells.

The neuropil of dentate nucleus contains axonal collaterals from Purkinje cells forming synapses with dendrites of the dentate neurons. The reduced synaptophysin reactivity in and around the dentate neurons indicates a decrease of presynapses as the possible secondary phenomenon of Purkinje cells loss, and enlarged dot-like staining pattern could indicate remaining enlarged presynapses. However, since we could also demonstrate apparent decrease in the number of dentate neurons, it is more likely that the inflammatory infiltrations may be primary cause of degeneration of synaptic terminals as well as the dentate neurons.

In the lung tumor tissue, we could detect CD8+ T cells invading the small cell carcinoma and closely adhering to the tumor cells, suggesting that T-cell mediated immune response to tumor antigen is cross-reactive to antigens in the central nervous system in PCD.

Based on our present findings, we suppose that dentate neurons and surrounding synaptic components should be considered as being primarily attacked in this PCD case. However, we could not exclude that involvement of Purkinje cells occurs first, followed by neuronal loss in the dentate nucleus in our PCD case. Therefore, further study focusing on dentate nucleus will be of great interest and will benefit understanding the T-cell mediated auto-immune neurological disorders like PCD.

Role of the funding source

Supported in part by the grant in aid for research on intractable diseases from the ministry of health, labor and welfare of Japanese government.

Acknowledgements

The authors thank Ms. Yoko Tomita for her excellent technical assistance and express our special thanks to Dr. Richard C. Wiggins of Environmental Protection Agency (US EPA) for his critical reading of this manuscript.

References

Anderson, N.E., Budde-Steffen, C., Wiley, R.G., Thurman, L., Rosenblum, M.K., Nadeau, S.E., Posner, J.B., 1988. A variant of the anti-Purkinje cell antibody in a patient with paraneoplastic cerebellar degeneration. Neurology 38, 1018–1026.

Albert, M.L., Darnell, J.C., Bender, A., Francisco, L.M., Bhardwaj, N., Darnell, R.B., 1998. Tumor-specific killer cells in paraneoplastic cerebellar degeneration. Nat Med. 4, 1321–1324.

Brieva-Ruíz, L., Diaz-Hurtado, M., Matias-Guiu, X., Márquez-Medina, D., Tarragona, J., Graus, F., 2008. Anti-Ri associated paraneoplastic cerebellar degeneration and breast cancer: An autopsy case study. Clin Neurol Neurosurg. 110, 1044–1046

Darnell, R.B., DeAngelis, L.M., 1993. Regression of small-cell lung carcinoma in patients with paraneoplastic neuronal antibodies. Lancet 341, 21–22.

Furneaux, H.M., Rosenblum, M.K., Dalmau, J., Wong, E., Woodruff, P., Graus, F., Posner, J.B., 1990. Selective expression of Purkinje-cell antigens in tumor tissue from patients with paraneoplastic cerebellar degeneration. N Engl J Med. 28, 1844–1851.

Greenlee, J.E., Parks, T.N., Jaeckle, K.A., 1993. Type IIa ('anti-Hu') antineuronal antibodies produce destruction of rat cerebellar granule neurons in vitro. Neurology 43, 2049–2054.

Giometto, B., Marchiori, G.C., Nicolao, P., Scaravilli, T., Lion, A., Bardin, P.G., Tavolato, B., 1997. Sub-acute cerebellar degeneration with anti-Yo autoantibodies: immunohistochemical analysis of the immune reaction in the central nervous system. Neuropathol Appl Neurobiol 23, 468–744.

Graus, F., Keime-Guibert, F., Reñe, R., Benyahia, B., Ribalta, T., Ascaso, C., Escaramis, G., Delattre, J.Y., 2001. Anti-Hu-associated paraneoplastic encephalomyelitis: analysis of 200 patients. Brain 124, 1138–1142.

Henson, R.A., Urich, H., 1982. Cortical cerebellar degeneration. Cancer and the Nervous System. Blackwell, pp. 346–367.

Hormigo, A., Dalmau, J., Rosenblum, M.K., River, M.E., Posner, J.B., 1994. Immunological and pathological study of anti-Ri-associated encephalopathy. Ann Neurol. 36, 896–902.

Liu, S., Tunkel, R., Lachmann, E., Nagler, W., 2000. Paraneoplastic cerebellar degeneration as the first evidence of cancer: a case report. Arch Phys Med Rehabil. 81, 834–836.

Posner, J.B., 1993. Paraneoplastic cerebellar degeneration. Can J Neurol Sci. 20 S117-22 Suppl. (Review).

Rosenblum, M.K., 1993. Paraneoplastic and autoimmunologic injury of the nervous system: the anti-Hu syndrome. Brain Pathol 3, 199–212.

Sillevis Smitt, P., Grefkens, J., de Leeuw, B., van den Bent, M., van Putten, W., Hooijkaas, H., Vecht, C., 2002. Survival and outcome in 73 anti-Hu positive patients with paraneoplastic encephalomyelitis/sensory neuronopathy. J Neurol. 249, 745–753.

Shams'ili, S., Grefkens, J., de Leeuw, B., van den Bent, M., Hooijkaas, H., van der Holt, B., Vecht, C., Sillevis Smitt, P., 2003. Paraneoplastic cerebellar degeneration associated with antineuronal antibodies: analysis of 50 patients. Brain 126, 1409–1418.

Tanaka, M., Tanaka, K., Tokiguchi, S., Shinozawa, K., Tsuji, S., 1999. Cytotoxic T cells against a peptide of Yo protein in patients with paraneoplastic cerebellar degeneration and anti-Yo antibody. J Neurol Sci. 15, 28–31.

Verschuuren, J., Chuang, L., Rosenblum, M.K., Lieberman, F., Pryor, A., Posner, J.B., Dalmau, J., 1996. Inflammatory infiltrates and complete absence of Purkinje cells in anti-Yo-associated paraneoplastic cerebellar degeneration. Acta Neuropathol. (Berl) 91, 519–525.

Astrocytic necrosis is induced by anti-aquaporin-4 antibody-positive serum

Makoto Kinoshita[a], Yuji Nakatsuji[a], Masayuki Moriya[a], Tatsusada Okuno[b], Atsushi Kumanogoh[b], Misa Nakano[c], Toshiyuki Takahashi[d], Kazuo Fujihara[e], Keiko Tanaka[f] and Saburo Sakoda[a]

Neuromyelitis optica (NMO) is an inflammatory demyelinating disease of the central nervous system, and humoral immunity is suggested to play an important role in the pathogenesis. The identification of an anti-aquaporin-4 antibody (AQP4-Ab, neuromyelitis optica immunoglobulin G) in the sera of patients with NMO has led to the investigation on the pathogenicity of the autoantibody. Recent immunohistological analyses revealed the primary loss of AQP4 on astrocytes and complement deposition in active lesions of NMO. In this report, we show that astrocytes are susceptible to sera from AQP4-Ab-positive patients and undergo necrosis in a complement-dependent manner. Our results suggest the primary pathogenic role of AQP4-Ab in NMO. ***NeuroReport*** **20:508–512 © 2009 Wolters Kluwer Health | Lippincott Williams & Wilkins.**

NeuroReport 2009, 20:508–512

Keywords: aquaporin-4, astrocyte, complement, multiple sclerosis, necrosis, neuromyelitis optica

[a]Departments of Neurology, Osaka University Graduate School of Medicine, [b]Immunopathology, Research Institute for Microbial Diseases, Osaka University, [c]Department of Neurology, Toyonaka Municipal Hospital, Osaka, [d]Departments of Neurology, [e]Multiple Sclerosis Therapeutics, Tohoku University Graduate School of Medicine, Sendai and [f]Department of Neurology, Kanazawa Medical University, Ishikawa, Japan

Correspondence to Associate Professor Yuji Nakatsuji, MD, PhD, Department of Neurology, Osaka University, Graduate School of Medicine, 2-2 Yamadaoka, Suita, Osaka 565-0871, Japan
Tel: +81 6 6879 3571; fax: +81 6 6879 3579;
e-mail: yuji@neurol.med.osaka-u.ac.jp

Received 24 September 2008 accepted 8 October 2008

Introduction

Neuromyelitis optica (NMO) is an inflammatory demyelinating disease of the central nervous system (CNS). Recurrent attacks of optic neuritis and myelitis are the hallmarks of both NMO and multiple sclerosis (MS), and therefore it has been debated whether NMO is a variant of MS or a separate disease [1–4]. The identification of a highly specific serum autoantibody, neuromyelitis optica immunoglobulin G (NMO-IgG) [1], in patients with NMO has led to investigation on the pathogenicity of the antibody [3–6]. NMO-IgG specifically binds to aquaporin-4 (AQP4), which is the most abundant water channel in the CNS, and is highly expressed at the perivascular endfeet of astrocytes [7]. Perivascular deposits of immunoglobulin and complement are characteristic to the pathology of NMO, indicating deregulated humoral immunity [3,4,8]. Recent immunohistological studies revealed the loss of AQP4 and glial fibrillary acidic protein with relatively preserved myelin basic protein in the active lesions of NMO [3,4]. Although these observations suggest that NMO-IgG-mediated astrocytic damage may be a pivotal pathogenic event in NMO, the evidence of the pathogenicity has not been shown. In this report, we showed a complement-dependent astrocytic necrosis induced by the sera of patients with NMO, which may account for the pathological changes observed in those patients.

Methods

Patients and anti-aquaporin-4 antibody assay

The sera were collected from six patients with clinically definite MS [9], six patients who tested positive for the anti-AQP4 antibody (AQP4-Ab), and six healthy volunteers (control subjects) after this study was approved by the ethics committee of Osaka University Hospital and informed consent was obtained from each patient. The six MS patients consisted of four patients with relapsing-remitting MS and two patients with secondary progressive MS. Four of the six AQP4-Ab-positive patients fulfilled the criteria for NMO [10]. The other two AQP4-Ab-positive patients had relapsing longitudinally extensive transverse myelitis without optic neuritis. The serum AQP4-Ab was tested according to the previously described method [11,12].

Cell isolation and viability assay

Primary astrocytes were obtained from Sprague–Dawley rats as previously described [13]. Experimental procedures were approved by the Institutional Animal Care and Use Committee of Osaka University Graduate School of Medicine. For the inactivation of complement, the patients' sera were incubated at 56°C for 30 min. Rabbit complement (Cappel, Solon, Ohio, USA) was used at the final concentration of 2% for the additional complement assay. The viability of the cells was assessed by

0959-4965 © 2009 Wolters Kluwer Health | Lippincott Williams & Wilkins

DOI: 10.1097/WNR.0b013e32832776f4

4-[3-(2-methoxy-4-nitrophenyl)-2-[4-nitrophenyl]-2H-5-tetrazolio]-1,3-benzene disulfonate sodium salt (WST-8) assay using a Cell Counting Kit-8 (Dojin East, Tokyo, Japan). For the assessment of astrocytic cell death, astrocytes were incubated with annexin V-FLUOS labeling reagent and propidium iodide (PI) (Roche, Penzberg, Germany).

Silencing effects of aquaporin-4

AQP4-specifc and control small interfering RNAs (siRNAs) were synthesized according to the previous report [14], and the transfection was performed using RNAiMAX (Invitrogen, Carlsbad, California, USA). Specific silencing was examined by western blot analysis. The blots were incubated with the anti-AQP4 antibody (1:500; Santa Cruz Biotechnology Inc., Santa Cruz, California, USA), then with a peroxidase-conjugated secondary antibody. The bands were visualized using an enhanced chemiluminescent detection system (ECL-Plus; Amersham, Buckinghamshire, UK).

Immunocytochemistry

Astrocytes, after a 1-h incubation with 10% heat-inactivated sera at 4°C, were labeled by the anti-human IgG1 antibody (Sigma-Aldrich, St Louis, Missouri, USA), followed by fixation with 4% paraformaldehyde in PBS. For C5b-9 staining, astrocytes were incubated with 5% sera for 2 h at 37°C, followed by fixation with ice-cold acetone and incubated with the anti-C5b-9 antibody (Abcam, Tokyo, Japan) overnight at 4°C. The astrocytes were then incubated with a biotin-conjugated secondary antibody followed by a second incubation with Alexa Fluor 488-conjugated streptavidin (Molecular Probes, Eugene, Oregon, USA).

Statistics

One-way analysis of variance and Bonferroni's multiple comparison tests were used for the statistical analysis.

Results

Aquaporin-4 antibody-positive serum decreases the astrocytic viability

To investigate the possible pathogenic role of AQP4-Ab, astrocytes were exposed to the sera from healthy volunteers, patients with MS, and patients with NMO spectrum disorders who harbor AQP4-Ab (collectively termed as NMO in this study) for 6 h. The cells

Fig. 1

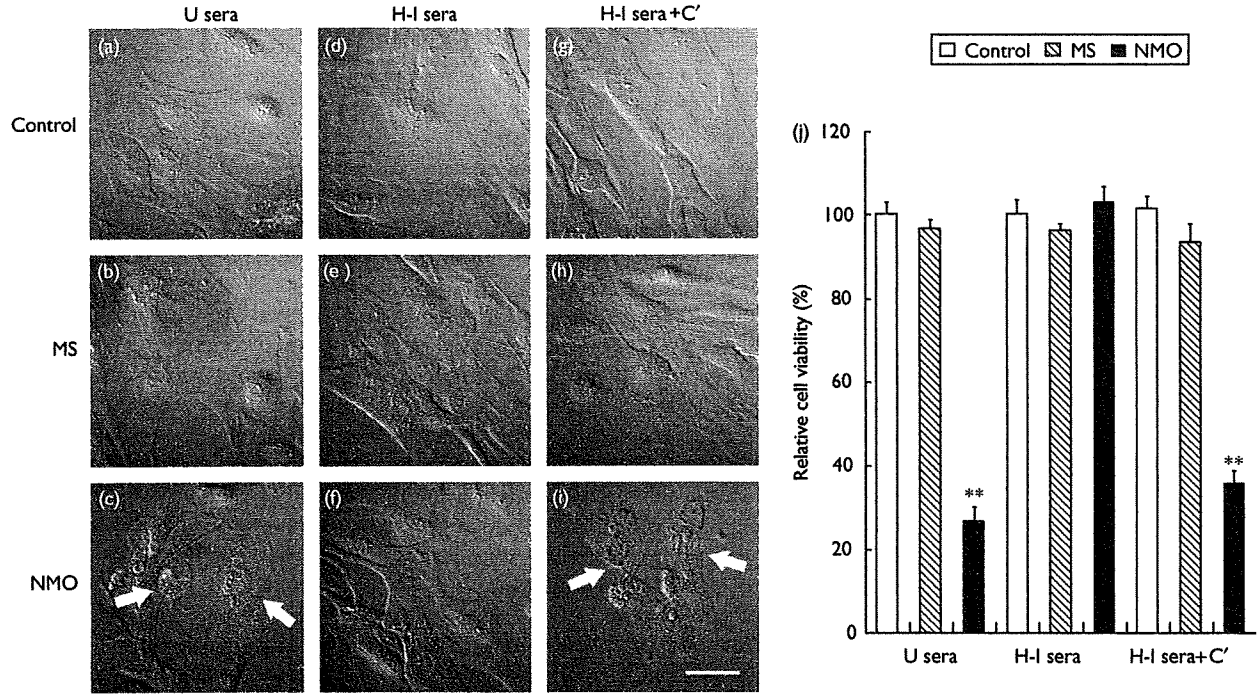

Neuromyelitis optica (NMO) patients' sera induce astrocytic cell damage in a complement-dependent manner. Astrocytes were incubated with 10% sera from the control, multiple sclerosis (MS), or NMO patients in 10% fetal bovine serum-Dulbecco's modified Eagle's medium for 6 h. (a–i) Differential interference contrast micrographs are shown. (a–c) Astrocytes were incubated with untreated sera (U sera). NMO sera induced cellular swelling and formation of a balloon-like structure of astrocytes (arrows), whereas such morphological changes were rarely seen with control or MS sera. (d–f) Morphological changes were not observed with heat-inactivated sera (H-I sera). (g–i) Complement addition to the heat-inactivated sera (H-I sera + C′) restored the toxic effect of NMO sera (arrows). Scale bar=40 μm. (j) The relative cell viability compared with the control group ($n=6$ per group) assessed by 4-[3-(2-methoxy-4-nitrophenyl)-2-[4-nitrophenyl]-2H-5-tetrazolio]-1,3-benzene disulfonate sodium salt assay is shown. Each column represents the mean ± SEM. $^{**}P<0.01$ for NMO versus control and MS groups.

incubated with NMO sera exhibited cellular swelling and formation of a balloon-like structure, thus suggesting astrocytic cell damage (Fig. 1c). In contrast, such morphological changes were rarely observed in astrocytes incubated with control or MS sera (Fig. 1a and b). WST-8 assay showed a decrease of approximately 70% in the viability of astrocytes incubated with 10% NMO sera (Fig. 1j). As the pathogenic effect of NMO serum on astrocytes was suggested, we next investigated an involvement of complement activation. Heat-inactivated sera from all three groups did not exhibit any morphological changes in astrocytes or a decrease in cell viability (Fig. 1d, e, f and j). We further examined whether an addition of complement to the heat-inactivated sera could restore the toxic effect, and a decreased cell viability with the same morphological changes were observed in astrocytes incubated with NMO sera (Fig. 1i and j). Thus, these results suggest that NMO sera are harmful to astrocytes and that the activation of complement is necessary for its toxicity.

Fig. 2

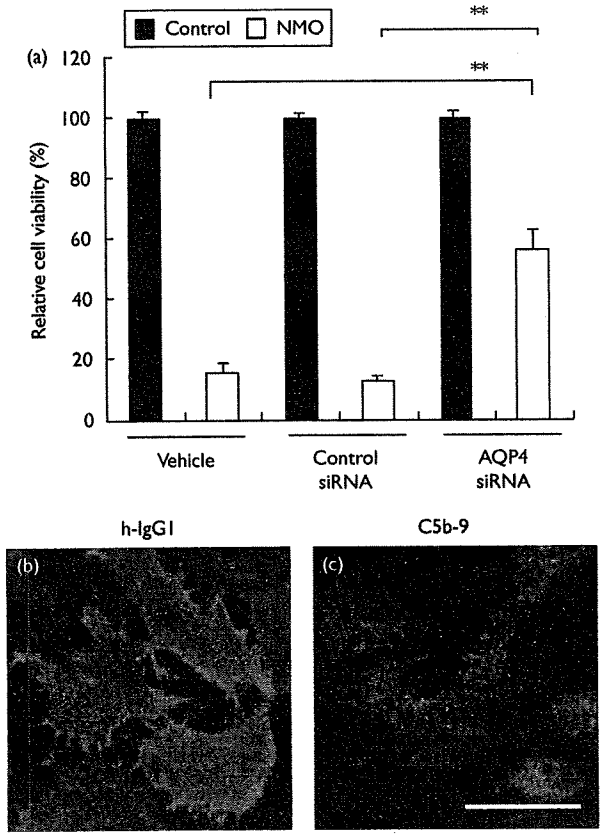

Aquaporin-4 (AQP4) is the target of sera from neuromyelitis optica (NMO) patients. (a) Downregulation of AQP4 restored the viability of astrocytes. Two days after the transfection with small interfering RNA (siRNA), astrocytes were incubated with 10% sera from the control or NMO group for 6 h in 1% fetal bovine serum-Dulbecco's modified Eagle's medium. The relative cell viability compared with the control group ($n=6$ per group) assessed by 4-[3-(2-methoxy-4-nitrophenyl)-2-[4-nitrophenyl]-2H-5-tetrazolio]-1,3-benzene disulfonate sodium salt assay is shown. Each column represents the mean ± SEM. (b) Astrocytes were incubated with 10% heat-inactivated sera from the control or NMO group for 1 h. Positive human IgG1 (H-IgG1) staining (green) was observed only with astrocytes incubated with NMO sera. (c) Astrocytes were incubated with 5% untreated sera from the control or NMO group for 2 h at 37°C. Positive C5b-9 staining (green) was observed only with astrocytes incubated with NMO sera. Scale bar = 40 μm. $^{**}P<0.01$.

Immunoglobulins in AQP4-Ab-positive serum bind to AQP4 on astrocytes and activate the complement pathway

To ascertain whether AQP4 is the critical target molecule in astrocytic damage induced by AQP4-Ab-positive sera, we downregulated the expression of AQP4 using siRNA. Successful knockdown of the AQP4 protein was confirmed by western blot analysis (data not shown). Then, the astrocytes were incubated with 10% sera from the control or NMO group for 6 h. WST-8 assay showed significant restoration of the cell viability in astrocytes transfected with AQP4-specific siRNA, but not with the transfection reagent alone (vehicle) or control siRNA (Fig. 2a). When the astrocytes were labeled with the anti-human IgG1 antibody, immunofluorescent staining was detected only in astrocytes incubated with NMO sera (Fig. 2b). Furthermore, immunoreactivity of C5b-9 was also detected only in astrocytes exposed to NMO sera (Fig. 2c). These results strongly suggest that the critical molecule targeted by the AQP4-Ab-positive serum is AQP4 itself and that the activation of classical complement pathway occurs on astrocytes.

Astrocytic necrosis but not apoptosis is induced by AQP4-Ab-positive serum

As the astrocytic cell damage was suggested by both the morphological changes and the decreased cell viability, we next performed examinations to elucidate whether the cell death is mediated by necrosis or apoptosis. Astrocytes were labeled with annexin V and PI after being incubated with 10% sera from the control, MS, or NMO group for 4 h. Most of the morphologically changed astrocytes incubated with NMO sera were double labeled with annexin V and PI (Fig. 3a). Cell counting showed that as many as 80% of the astrocytes incubated with NMO sera were double labeled, whereas the annexin V single-positive cells accounted for less than 2% (Fig. 3b). These results suggest that the astrocytic cell death induced by NMO serum is necrosis, not apoptosis.

Discussion

Astrocytes are endowed with many complement-regulatory proteins, and they are reported to be substantially resistant to cell lysis [15,16]. However, our results show the unexpected susceptibility of astrocytes to complement-mediated cell death. It is reported that astrocytes are susceptible to cell lysis in the presence of a complement-fixing antibody [15]. Complement-dependent

Fig. 3

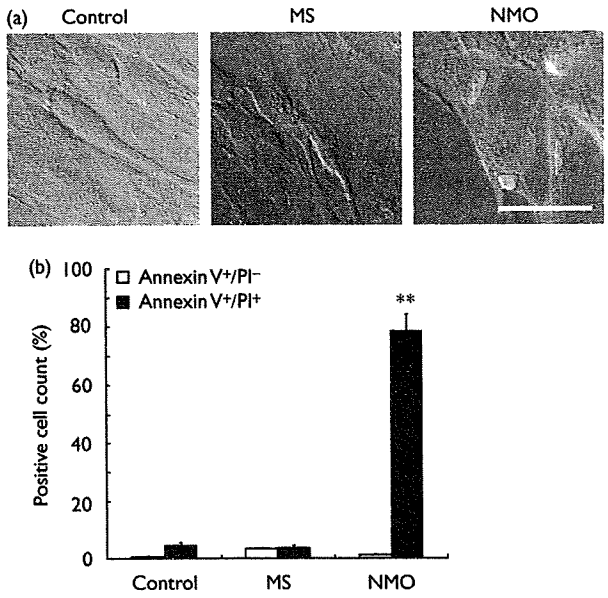

Neuromyelitis optica (NMO) sera induce necrosis of astrocytes. Annexin V and propidium iodide (PI) staining was performed after the 4-h incubation with 10% untreated sera from the control, multiple sclerosis (MS), or NMO group in 10% fetal bovine serum-Dulbecco's modified Eagle's medium. (a) Micrographs of astrocytes stained with annexin V (green) and PI (red). Merged images overlapped with light microscopy images are shown. Scale bar=40 μm. (b) The number of cells positively stained with annexin V and/or PI was counted. The results are shown as the percentage of the immunoreactive cells in the total population. Each column represents the mean±SEM. $^{**}P<0.01$ for NMO versus control and MS groups.

astrocytic cell death by the anti-GluR3 antibody is also reported [17]. As AQP4-Ab predominantly belongs to a major complement-activating IgG subclass [5], it is plausible that AQP4-Ab activates classical complement pathway on astrocytes. In addition, as the downregulation of AQP4 expression restored the viability of the astrocytes (Fig. 2a), the critical molecule targeted by the sera of NMO patients is strongly suggested to be AQP4 itself. These results suggest that AQP4-Ab in the sera of NMO patients binds specifically to AQP4, which then activates the classical complement cascade and leads to the cell damage. With regard to the complement-mediated cell death, apart from lysing cells, C5b-9 is also reported to be an important factor for regulating the initiation and inhibition of apoptosis in target cells [16,18]. However, both the rapid formation of a balloon-like structure and the double-labeled astrocytes with annexin V/PI suggested the classical lytic role of C5b-9 in dying cells [19], and this result is consistent with the necrotic changes observed in the lesions of NMO [3,4,8].

As AQP4-Ab predominantly exists in the serum rather than the cerebrospinal fluid [6], the question as to how the peripheral antibody gains access to the parenchyma of the CNS arises. Vasculocentric deposition of complement is reported in NMO [3,4,8], which is in contrast to parenchymal deposition in pattern-II MS [20]. Together with our finding that astrocytes are unexpectedly susceptible to the patient's serum, it is possible that when the antibody, even in a small amount, reaches the astrocytic endfeet, it would deteriorate the integrity of the blood–brain barrier and lead to further tissue destruction. As our findings are based on in-vitro experiments, establishment of the appropriate animal model should be of great assistance to elucidate the precise underlying mechanisms of NMO.

Conclusion

In this study, we have shown that astrocytes are unexpectedly susceptible to complement-mediated cell death in the presence of AQP4-Ab. Our results are consistent with the necrotic changes observed in the lesions of NMO and suggest the primary pathogenic role of AQP4-Ab in those patients.

Acknowledgements

This study was supported in part by the Program for Promotion of Fundamental Studies in Health Sciences of the National Institute of Biomedical Innovation (Y.N. and A.K.) and by the Health and Labour Sciences Research Grants for research on intractable diseases from the Ministry of Health, Labour and Welfare of Japan. None of the authors have any financial interests related to this study.

References

1 Lennon VA, Wingerchuk DM, Kryzer TJ, Pittock SJ, Lucchinetti CF, Fujihara K, *et al.* A serum autoantibody marker of neuromyelitis optica: distinction from multiple sclerosis. *Lancet* 2004; **364**:2106–2112.
2 Matsuoka T, Matsushita T, Kawano Y, Osoegawa M, Ochi H, Ishizu T, *et al.* Heterogeneity of aquaporin-4 autoimmunity and spinal cord lesions in multiple sclerosis in Japanese. *Brain* 2007; **130**:1206–1223.
3 Misu T, Fujihara K, Kakita A, Konno H, Nakamura M, Watanabe S, *et al.* Loss of aquaporin 4 in lesions of neuromyelitis optica: distinction from multiple sclerosis. *Brain* 2007; **130**:1224–1234.
4 Roemer SF, Parisi JE, Lennon VA, Benarroch EE, Lassmann H, Bruck W, *et al.* Pattern-specific loss of aquaporin-4 immunoreactivity distinguishes neuromyelitis optica from multiple sclerosis. *Brain* 2007; **130**:1194–1205.
5 Hinson SR, Pittock SJ, Lucchinetti CF, Roemer SF, Fryer JP, Kryzer TJ, *et al.* Pathogenic potential of IgG binding to water channel extracellular domain in neuromyelitis optica. *Neurology* 2007; **69**:2221–2231.
6 Takahashi T, Fujihara K, Nakashima I, Misu T, Miyazawa I, Nakamura M, *et al.* Anti-aquaporin-4 antibody is involved in the pathogenesis of NMO: a study on antibody titre. *Brain* 2007; **130**:1235–1243.
7 Lennon VA, Kryzer TJ, Pittock SJ, Verkman AS, Hinson SR. IgG marker of optic-spinal multiple sclerosis binds to the aquaporin-4 water channel. *J Exp Med* 2005; **202**:473–477.
8 Lucchinetti CF, Mandler RN, McGavern D, Bruck W, Gleich G, Ransohoff RM, *et al.* A role for humoral mechanisms in the pathogenesis of Devic's neuromyelitis optica. *Brain* 2002; **125**:1450–1461.
9 Poser CM, Paty DW, Scheinberg L, McDonald WI, Davis FA, Ebers GC, *et al.* New diagnostic criteria for multiple sclerosis: guidelines for research protocols. *Ann Neurol* 1983; **13**:227–231.
10 Wingerchuk DM, Lennon VA, Pittock SJ, Lucchinetti CF, Weinshenker BG. Revised diagnostic criteria for neuromyelitis optica. *Neurology* 2006; **66**:1485–1489.
11 Tanaka K, Tani T, Tanaka M, Saida T, Idezuka J, Yamazaki M, *et al.* Anti-aquaporin 4 antibody in selected Japanese multiple sclerosis patients with long spinal cord lesions. *Mult Scler* 2007; **13**:850–855.

12 Takahashi T, Fujihara K, Nakashima I, Misu T, Miyazawa I, Nakamura M, *et al.* Establishment of a new sensitive assay for anti-human aquaporin-4 antibody in neuromyelitis optica. *Tohoku J Exp Med* 2006; **210**:307–313.
13 Nakatsuji Y, Miller RH. Density dependent modulation of cell cycle protein expression in astrocytes. *J Neurosci Res* 2001; **66**:487–496.
14 Nicchia GP, Frigeri A, Liuzzi GM, Svelto M. Inhibition of aquaporin-4 expression in astrocytes by RNAi determines alteration in cell morphology, growth, and water transport and induces changes in ischemia-related genes. *FASEB J* 2003; **17**:1508–1510.
15 Rogers CA, Gasque P, Piddlesden SJ, Okada N, Holers VM, Morgan BP. Expression and function of membrane regulators of complement on rat astrocytes in culture. *Immunology* 1996; **88**:153–161.
16 Rus H, Cudrici C, David S, Niculescu F. The complement system in central nervous system diseases. *Autoimmunity* 2006; **39**:395–402.
17 Whitney KD, McNamara JO. GluR3 autoantibodies destroy neural cells in a complement-dependent manner modulated by complement regulatory proteins. *J Neurosci* 2000; **20**:7307–7316.
18 Cole DS, Morgan BP. Beyond lysis: how complement influences cell fate. *Clin Sci (Lond)* 2003; **104**:455–466.
19 Krysko DV, Vanden Berghe T, D'Herde K, Vandenabeele P. Apoptosis and necrosis: detection, discrimination and phagocytosis. *Methods* 2008; **44**:205–221.
20 Lucchinetti C, Bruck W, Parisi J, Scheithauer B, Rodriguez M, Lassmann H. Heterogeneity of multiple sclerosis lesions: implications for the pathogenesis of demyelination. *Ann Neurol* 2000; **47**:707–717.

Journal of Neuroimmunology xxx (2009) xxx–xxx

Contents lists available at ScienceDirect

Journal of Neuroimmunology

journal homepage: www.elsevier.com/locate/jneuroim

Short communication

Identification of binding sites for anti-aquaporin 4 antibodies in patients with neuromyelitis optica

T. Tani [a], K. Sakimura [b], M. Tsujita [c], T. Nakada [c], M. Tanaka [d], M. Nishizawa [a], K. Tanaka [a,e,*]

[a] Department of Neurology, Brain Research Institute, Niigata University, Niigata Japan
[b] Department of Cellular and Neurobiology, Brain Research Institute, Niigata University, Niigata, Japan
[c] Center for Integrated Human Brain Science, Brain Research Institute, Niigata University, Niigata, Japan
[d] Department of Neurology, Utano National Hospital, Kyoto, Japan
[e] Kanazawa Medical University, Ishikawa, Japan

ARTICLE INFO

Article history:
Received 29 December 2008
Received in revised form 4 March 2009
Accepted 1 April 2009
Available online xxxx

Keywords:
Anti-aquaporin-4 antibodies
NMO
Chimera mutant AQP4
Epitope
Extracellular domain

ABSTRACT

Objective: Anti-aquaporin 4 antibodies (AQP4-Ab) are specifically detected in patients with neuromyelitis optica. To investigate the role of AQP4-Ab, we examined the antibody binding epitope using human and mouse mutant AQP4. *Methods:* We constructed human and mouse amino acid substitution AQP4 mutants and compared the reactivity with wild-form of human, mouse and rat AQP4. *Results:* The decreased intensity of AQP4-Ab staining with mouse AQP4 was recovered to that of human AQP4 with the mouse mutant A228E for 9 of the 10 sera. *Conclusions:* The third extracellular loop of AQP4 is considered to be the major epitope for AQP4-Ab in NMO.

1. Introduction

Anti-aquaporin 4 antibodies (AQP4-Ab) are specifically detected in patients with neuromyelitis optica (NMO). We previously established a method for immunofluorescence detection of NMO-IgG in cryostat sections of rat brain tissue and human embryonic kidney (HEK-293) cells transfected with human AQP4 using AQP4-Ab following Lennon et al. with some modifications (Lennon et al., 2004, 2005). We subsequently examined the presence of NMO-IgG/AQP4-Ab in a large cohort of Japanese NMO patients and confirmed that NMO-IgG/AQP4-Ab is an excellent marker for NMO (Tanaka et al., 2007).

However, it remains unclear whether AQP4-Ab binds directly to AQP4-expressing cells during the development of NMO lesions in the central nervous system (CNS). To further investigate the molecular mechanisms underlying the activity of AQP4-Ab, we examined its binding site using human and mouse AQP4 mutants, comparing with wild form human, mouse and rat AQP4.

2. Materials and methods

2.1. Construction of plasmid vectors containing human and mouse AQP4

cDNA encoding human aquaporin 4 (AQP4M23 isoform; GenBank accession number U63623 (Lu et al., 1996)) was cloned, cDNA synthesized from human brain total RNA and full-length cDNA of M23 isoform inserted into the XbaI site of the pEF-BOS expression vector (BOS-hAQP4(b)) as previously described (Mizushima and Nataga, 1990). Mouse AQP4 was cloned (GenBank accession number AF469168) and an expression vector containing full-length cDNA constructed (BOS-mAQP4). Rat AQP4 expressing vector is generously gifted from Dr. K. Tani, Kyoto University.

2.2. Mutant AQP4 construction

We have previously shown that NMO patient serum reacts with both M1 and M23 splice variants of human AQP4. Thus, we used the M23 sequence in this study. DNA sequences for human and mouse AQP4 show 95% homology and demonstrate only 15 amino acid differences. If AQP4-Ab recognizes the AQP4 extracellular domain, only 4 amino acids differences occur between human and mouse and 3 differences between human and rat (Fig. 1). Given that the nucleotide positions Ser 62 and Asn 64 are close to each other, we constructed three mouse AQP4 mutants by substituting each amino

* Corresponding author. Department of Neurology, Kanazawa Medical University, 1-1 Daigaku, Uchinada-machi, Kahoku-gun, Ishikawa 920-0293, Japan. Tel.: +81 76 286 2211; fax: +81 76 286 3259.
E-mail address: k-tana20@kanazawa-med.ac.jp (K. Tanaka).

0165-5728/$ – see front matter © 2009 Elsevier B.V. All rights reserved.
doi:10.1016/j.jneuroim.2009.04.001

Please cite this article as: Tani, T., et al., Identification of binding sites for anti-aquaporin 4 antibodies in patients with neuromyelitis optica, J. Neuroimmunol. (2009), doi:10.1016/j.jneuroim.2009.04.001

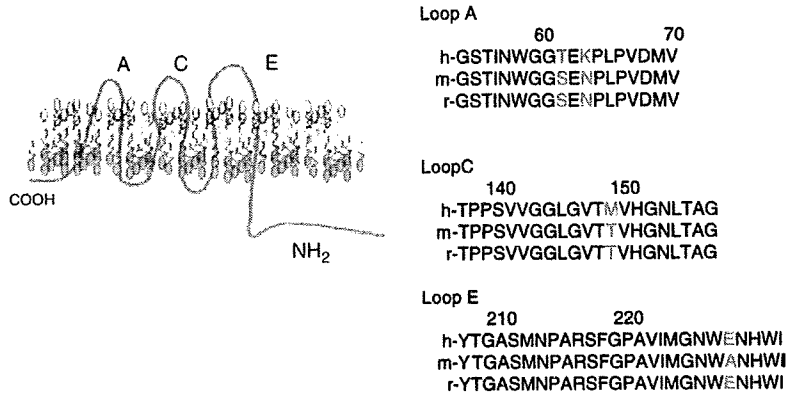

Fig. 1. Structure of AQP4. The positions of amino acid difference between human, mouse and rat are shown with red color. (cited from Graber et al., 2008)

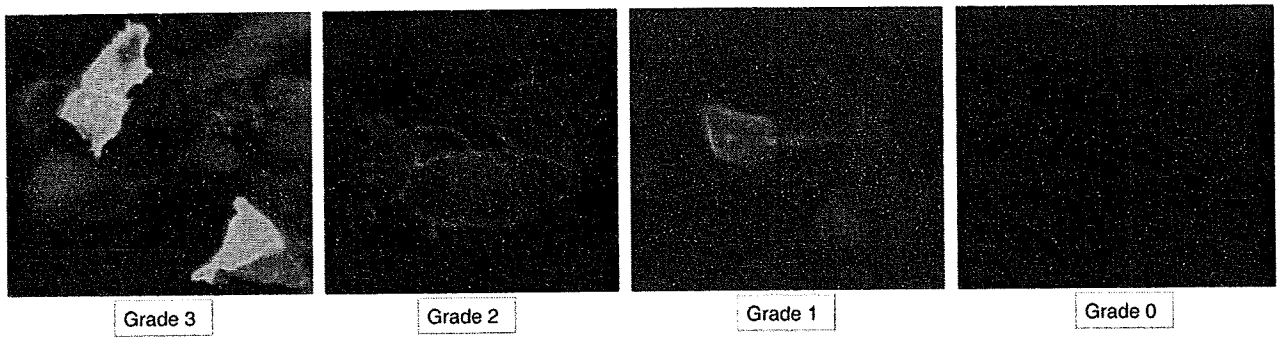

Fig. 2. Grading of immunofluorescence intensity. Immunofluorescence staining intensity was graded as: 3, staining intensity was similar to the original w-hAQP4 assay; 2, linear staining of the cell margin but weaker than 3; 1, weak staining without clear linear pattern; and 0, negative stain.

acid in human AQP4 to mouse (S62T/N64K, T149M and A228E) using the KOD Plus Mutagenesis kit (TOYOBO Osaka). We also produced human AQP4 cDNAs that had been substituted with mouse amino acids (T62S/K64N, M149T and E228A). The DNA sequence of each mutant was confirmed by DNA sequencing.

2.3. Transfection of HEK-293 cells

HEK-293 cells were seeded at 4×10^4 cells in poly-l-lysine-coated 8-well chamber slides (BD BioCoat) and cultured overnight in Dulbecco's modified Eagle's medium (DMEM) containing 10% fetal calf serum (FCS). The cells were then transfected with M23 wild-form human AQP4 (w-hAQP4), wild-form mouse AQP4 (w-mAQP4), wild-form rat AQP4 (w-rAQP4), mouse AQP4 mutant (S62T/N64K, T149M, A228E) or human AQP4 mutant (T62S/K64N, M149T, E228A) expression vectors or a control empty vector using Lipofectamine (Invitrogen).

2.4. Anti-AQP4 antibody containing sera

Sera from 10 patients that contained high AQP4-Ab titers (>1:25,600) were used as the primary antibody for immunofluorescence staining. Sera from 3 healthy individuals were used as a control. To examine expression of mouse AQP4 in the HEK-293 cells, an antibody raised in rabbit following immunization with C-terminal mouse AQP4 peptides, which is known to specifically react with mouse AQP4 was used.

2.5. Immunohistochemistry

Twenty-four hours following transfection, HEK-293 cells were fixed in 4% paraformaldehyde in 0.1 M phosphate-buffered saline (PBS, pH 7.4) for 20 min. Non-specific binding was blocked with 10% goat serum/PBS, and cells were incubated with patient sera (1:100) or anti-mouse AQP4 sera (1:20) for 60 min at room temperature, and then with FITC-conjugated rabbit anti-human IgG (BD Biosciences) or FITC-mouse anti-rabbit IgG (Santa Cruz Biotechnology) for 30 min. SlowFade Gold anti-fade reagent (Molecular Probes) was then applied to the slides and the staining observed via fluorescence microscopy.

2.6. Immunostaining analysis

Positively-stained cells observed in 10 fields (×100) were graded into 3 groups in accordance to their pattern of staining: 3, similar staining to the original w-hAQP4 assay; 2, linear staining at the cell margin, but weaker than 3; 1, limited staining without clear linear patterning, and 0, negative stain. Grading was undertaken by two independent investigators. (Fig. 2)

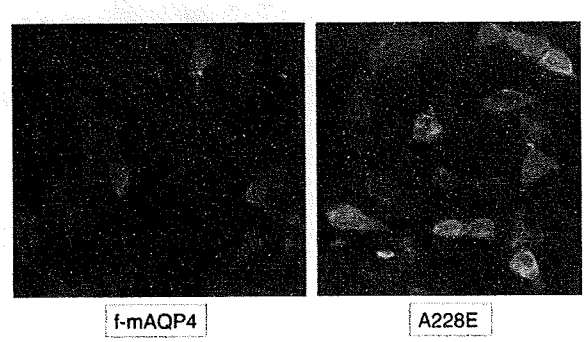

Fig. 3. AQP4-Ab from NMO patient weakly recognized w-mAQP4. The staining intensity was recovered with E228A mutant.

Please cite this article as: Tani, T., et al., Identification of binding sites for anti-aquaporin 4 antibodies in patients with neuromyelitis optica, J. Neuroimmunol. (2009), doi:10.1016/j.jneuroim.2009.04.001

Table 1
Staining intensity for each mutant with 10 sera from AQP4-Ab positive NMO patients.

Patient No.	wild mAQP4	S62T/N64K mAQP4	T149M mAQP4	A228E mAQP4	T62S/K64N hAQP4	M149T hAQP4	E228A hAQP4	wild hAQP4
1	0	1	1	3	3	3	3	3
2	1	2	1	2	3	3	3	3
3	1	2	2	3	3	3	3	3
4	1	0	1	1	1	1	1	3
5	1	2	2	3	3	3	3	3
6	1	2	2	3	3	3	3	3
7	1	0	1	2	3	3	3	3
8	1	1	1	2	3	3	2	3
9	1	1	1	2	3	3	2	3
10	0	1	0	2	3	3	3	3

Positively-stained cells observed in 10 fields (x100) were graded into 4 groups in accordance to their pattern of staining: 3, similar staining to the original w-hAQP4 assay; 2, linear staining at the cell margin, but weaker than 3; 1, limited staining without clear linear patterning, and 0, negative stain. Grading was undertaken by two independent investigators.

2.7. Immunohistochemistry using rat or mouse brain tissues

The cryostat sections from rat or mouse cerebrum, cerebellum and spinal cord were air dried, fixed in cold acetone for 10 min., blocked with 10% gout serum containing PBS, incubated with AQP4-Ab positive NMO sera and then FITC-anti-human IgG as previously shown (Tanaka et al., 2007).

3. Results

The expression of AQP4 proteins on the surface of HEK-293 cells transfected with human M23 isoform and mouse and rat AQP4 cDNAs (w-hAQP4 or w-mAQP4, w-rAQP4) or mutant AQP4 expression vectors was examined using AQP4-Ab positive patients' sera (NMO sera) or antibodies against mouse or rat AQP4. HEK-293 transfected with each of the wild type or AQP4 mutant was stained on the cell surface. In contrast, sera from healthy individuals or mouse did not react with transfected cells, or the cells transfected with empty vector.

NMO sera with high AQP4-Ab titers reacted weakly with the cells expressing w-mAQP4. The staining intensity for 9 of the 10 sera was recovered to those of w-hAQP4 when the mouse AQP4 mutant A228E was used and was partly recovered with T149M mutant, but not with S62T/N64K mutant (Fig. 3). Only 3 of the sera showed a reduction in staining intensity with mutant E228A of hAQP4. In contrast, most of the sera except one did not show staining decrement with the mutant T62S/K64N and M149T compared with w-hAQP4 (Table 1). The w-rAQP4 expressing cells showed more intense staining than w-hAQP4 with all sera examined (data not shown).

The immunostaining of rat and mouse CNS tissues with NMO sera showed more intense staining with rat tissue than mouse tissue (Fig. 4).

4. Discussion

AQP4 is a major water channel located on the astrocytic endfeet at the glia limitans surrounding the ventricles and endothelial cell basal membranes in the CNS (Verkman, 2005). AQP4 is thought to regulate brain edema (Manley et al., 2000; Papadopoulos et al., 2004) and is also a known target antigen for NMO serum antibodies (Lennon et al.2005). Although several lines of evidence exist, it remains unclear as to whether AQP4-Ab is directly related to NMO lesion development.

As NMO is prevalent in Japan, we established an AQP4-Ab detection system. Prior to establishing this system, we first attempted to detect AQP4-Ab using solubilized AQP4 protein as an antigen for western blotting. We also produced fragmented recombinant proteins containing each of the AQP4 extracellular domains. However, these products failed to be recognized by NMO sera. Thus, we speculated that AQP4 may be recognized as an antigen in tertiary preserved structures and so we established a detection system using HEK-293 cells (Lennon et al., 2005; Tanaka et al., 2007).

We also examined reactivity of AQP4-Ab with mouse AQP4, which resulted in weaker reactivity than human AQP4-expressing cells, even though the AQP4 amino acid sequence is highly homologous between human and mouse.

Based on algorithm analysis of the AQP4 sequence, AQP4 demonstrates three extracellular loops that connect 6 alpha helices that span the membrane (Jung et al., 1994). AQP4 is associated with several transmembrane proteins including α and β-dystroglycan, dystrophin isoform Dp71, and syntrophin (Neely et al., 2001). Single nucleotide substitutions may change the AQP4 structure in relation to its associated proteins, which might in turn alter the AQP4 antibody reactivity between human, rat and mouse.

Therefore, we next produced chimera AQP4 mutants constructed by exchanging each of the amino acids located at the extracellular

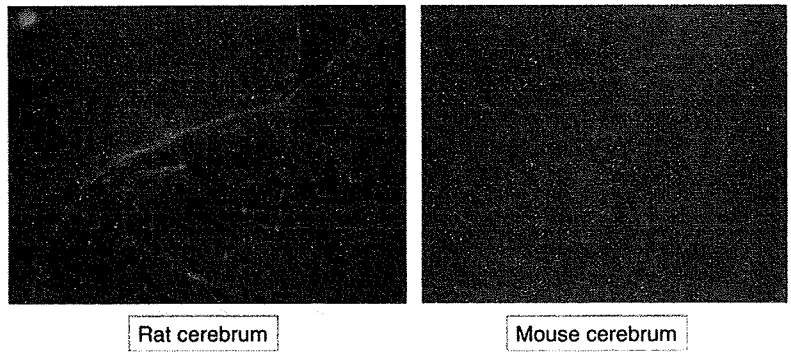

Fig. 4. Indirect immunofluorescence staining. The AQP4-Ab positive sera from NMO patients reacted more intensely with cryostat sections of rat cerebrum than mouse cerebral tissue.

Please cite this article as: Tani, T., et al., Identification of binding sites for anti-aquaporin 4 antibodies in patients with neuromyelitis optica, J. Neuroimmunol. (2009), doi:10.1016/j.jneuroim.2009.04.001

domain and compared with each of the human, mouse, and rat wild-form AQP4. NMO sera reacted strongly with w-hAQP4 showed weak binding with w-mAQP4 but recovered its reactivity to levels of w-hAQP4 when mouse AQP4 mutant A228E was used. That recovery was partial with mutant T149M and no recovery with S62T/N64K.

These results suggested that the major epitope of AQP4-Ab is located at the E-loop of human AQP4 around the position of amino acid no. 228.

In the present study, one of the sera did not recover its reactivity using A228E. This may be due to polyclonality of human NMO antibodies, resulting in different reactivity to AQP4 structures.

Most of the NMO sera reacted well with h-AQP4 substituted with the mouse amino acids T62S/K64N, M149T or E228A, though some showed reduction with E228A. It remains unclear as to why human mutant E228A, substituted with mouse amino acids did not show decreased staining as to mouse AQP4 level, although the reverse mutants of mouse AQP4 recovered their reactivity from clearly decreased levels with w-mAQP4. Since the structural expression of mutant AQP4 might be different from wild form, we also examined w-rAQP4 having one amino acid difference with mouse AQP4 on the loop E together with immunohistochemical staining of rat CNS tissue, that resulted intense staining with all of the sera. Looking at the amino acid difference of each of the extracellular loop between mouse, rat and human AQP4, our results suggested that NMO sera mainly recognize loop E of human AQP4 and loop E together with loop A and/or loop C with rat AQP4 that strengthen the reactivity of NMO sera with rat AQP4. Mouse AQP4 was recognized weakly because of loop E structure is different from human and rat. These also suggested that AQP4-Ab does not recognize one small linear sequence as its epitope, but instead recognizes polymerized structures and third extra-membranous domains that play a major role in maintaining a structure of human AQP4. In addition, the structure of rodent AQP4 may be regulated by further rules.

It is essential to determine the major epitopes of AQP4-Ab in order to produce an efficient NMO disease model, to study functional changes in the AQP4 water channel, to understand AQP4 structure on the cell surface and to develop therapy for NMO that will specifically block pathogenic peptide portions.

Acknowledgements

This study was supported in part by the Ministry of Education, Culture, Sports, Science and Technology, Japan, and a Neuroimmunological Disease Research Committee grant from the Ministry of Health, Labour and Welfare, Japan.

References

Graber, D., Levy, M., Kerr, D., Wade, W.F., 2008. Neuromyelitis optica pathogenesis and aquaporin 4. J. Neuroinflammation 5, 1–21.

Jung, J.S., Preston, G.M., Smith, B.L., Guggino, W.B., Agre, P., 1994. Molecular structure of the water channel through aquaporin CHIP. The hourglass model. J. Biol. Chem. 269, 14648–14654.

Lu, M., Lee, M.D., Smith, B.L., Jung, J.S., Agre, P., Verdijk, M.A., Merlck, G., Rijss, J.P., Deen, P.M., 1996. The human AQP4 gene: definition of the locus encoding two water channel polypeptides in brain. Proc. Natl. Acad. Sci. U.S.A. 93, 10908–10912.

Lennon, V.A., Wingerchuk, D.M., Kryzer, T.J., Pittock, S.J., Lucchinetti, C.F., Fujihara, K., Nakashima, I., Weinshenker, B.G., 2004. A serum autoantibody marker of neuromyelitis optica: distinction from multiple sclerosis. Lancet 364, 2106–2112.

Lennon, V.A., Kryzer, T.J., Pittock, S.J., Verkman, A.S., Hinson, S.R., 2005. IgG marker of optic-spinal multiple sclerosis binds to the aquaporin-4 water channel. J. Exp. Med. 202, 473–477.

Manley, G.T., Fujimura, M., Ma, T., Noshita, N., Filiz, F., Bollen, A.W., Chan, P., Verkman, A.S., 2000. Aquaporin-4 deletion in mice reduces brain edema after acute water intoxication and ischemic stroke. Nat. Med. 6, 159–163.

Mizushima, S., Nagata, S., 1990. pEF-BOS, a powerful mammalian expression vector. Nucleic Acids Res. 18 (17), 5322.

Neely, J.D., Amiry-Moghaddam, M., Ottersen, O.P., Froehner, S.C., Agre, P., Adams, M.E., 2001. Syntrophin-dependent expression and localization of Aquaporin-4 water channel protein. Proc. Natl. Acad. Sci. U.S.A. 98, 14108–14113.

Papadopoulos, M.C., Manley, G.T., Krishna, S., Verkman, A.S., 2004. Aquaporin-4 facilitates reabsorption of excess fluid in vosIgenic brain edema. FASEB J. 18 (11), 1291–1293.

Tanaka, K., Tani, T., Tanaka, M., Saida, T., Idezuka, J., Yamazaki, M., Tsujita, M., Nakada, T., Sakimura, K., Nishizawa, M., 2007. Anti-aquaporin 4 antibody in Japanese multiple sclerosis with long spinal cord lesions. Mult. Scler. 13, 850–855.

Verkman, A.S., 2005. More than just water channels: unexpected cellular roles of aquaporins. J. Cell Sci. 118, 3225–3232.

Please cite this article as: Tani, T., et al., Identification of binding sites for anti-aquaporin 4 antibodies in patients with neuromyelitis optica, J. Neuroimmunol. (2009), doi:10.1016/j.jneuroim.2009.04.001

J Neurol (2009) 256:1762–1764
DOI 10.1007/s00415-009-5175-6

LETTER TO THE EDITORS

Efficacy of tacrolimus in Sjögren's syndrome-associated CNS disease with aquaporin-4 autoantibodies

Taku Fukuda · Hirokazu Shiraishi · Tatsufumi Nakamura · Keiko Tanaka · Hideki Nakamura · Akira Tsujino · Yoshihiro Nishiura · Toshiro Yoshimura · Masakatsu Motomura · Katsumi Eguchi

Received: 15 December 2008 / Revised: 3 May 2009 / Accepted: 10 May 2009 / Published online: 26 May 2009

Sirs,

We present two patients with central nervous system (CNS) disease associated with Sjögren's syndrome (SjS) and positive for antiaquaporin-4 water channel autoantibodies (AQP4-Ab) who were treated successfully with tacrolimus. Tacrolimus is an immunosuppressant that acts as a calcineurin inhibitor and suppresses T helper 2 (Th2) cells [1]. Tacrolimus may also act as a neuroprotectant by reducing axonal and myelin damage, as shown in a mouse model of experimental autoimmune encephalomyelitis [2]. SjS is a chronic autoimmune disease characterized by lymphocytic infiltration of the exocrine glands. SjS-associated inflammation sometimes spreads into the CNS (CNS–SjS), occasionally mimics relapsing-remitting multiple sclerosis (MS), and inflammation often involves the brain, spinal cord, and optic nerve [3]. Neuromyelitis optica (NMO) is also a relapsing inflammatory disease of the CNS, characterized by severe attacks of optic nerve neuritis and longitudinally extensive transverse myelitis [4]. NMO is distinguished from MS by the presence of AQP4-Ab and differences in the distribution of inflammatory lesions and pathological findings. Combination therapy with a corticosteroid and azathioprine is the current standard treatment for preventing NMO relapse [5]; however, some patients are refractory to this therapy. Approximately 3% of patients with NMO have coexisting systemic lupus erythematosus (SLE) or SjS, and CNS–SjS patients with optic nerve neuritis or longitudinal myelitis (conditions called "NMO spectrum disorder") often present with positive findings for AQP4-Ab [4, 6, 7]. To our knowledge, this is the first reported assessment of tacrolimus in patients with CNS–SjS with AQP4-Ab. This treatment was approved by the ethical committee of our university, and the patients provided written informed consent.

A 48-year-old female (Patient 1, Fig. 1) was admitted to the hospital with rapidly progressive nausea, hiccups, dysphagia, and drowsiness. Magnetic resonance imaging (MRI) revealed T2 hyperintensities of the hypothalamus bilaterally and the dorsal medulla oblongata. After three courses of intravenous high-dose methylprednisolone (IHMP, 1 g/day for 3 days in one course), the patient recovered completely, except for mild dysphagia. One year after the first attack, she developed limb weakness. Laboratory test results revealed high levels of anti-Ro (SSA) antibodies and positive antinuclear antibody. The Schirmer test and the Saxon test revealed decreased salivary secretion (Table 1). She was diagnosed with CNS–SjS [8]. She experienced nine attacks during the entire disease course, and we started treatment with oral tacrolimus during her ninth admission. No recurrent attacks have been observed for 49 months since the start of this treatment.

T. Fukuda (✉) · H. Shiraishi · H. Nakamura · A. Tsujino · Y. Nishiura · M. Motomura · K. Eguchi
First Department of Internal Medicine,
Graduate School of Biomedical Sciences,
Nagasaki University, 1-7-1 Sakamoto,
Nagasaki 852-8501, Japan
e-mail: taku-ngs@umin.ac.jp

T. Nakamura
Department of Molecular Microbiology and Immunology,
Graduate School of Biomedical Sciences, Nagasaki University,
Nagasaki, Japan

K. Tanaka
Department of Neurology, Kanazawa Medical University,
Kanazawa, Japan

T. Yoshimura
School of Health Sciences, Nagasaki University,
Nagasaki, Japan

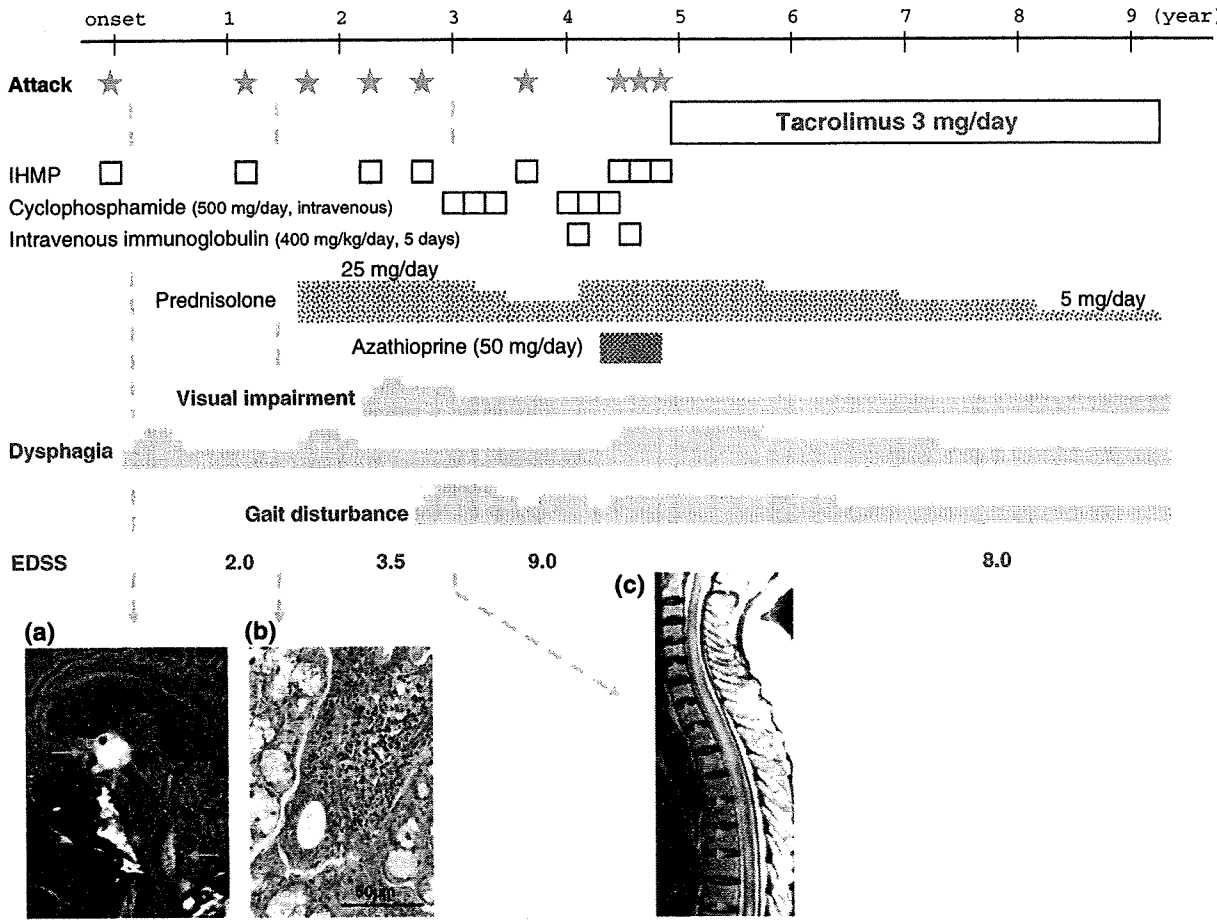

Fig. 1 Time course of relapse, therapies, symptoms, and images of Patient 1. *Stars* indicate attacks. The *thickness of each line* represents the severity of any symptom or the dose of drug. Nine attacks had occurred in spite of therapeutic approaches, and no attacks were observed after starting tacrolimus. **a** A sagittal fluid-attenuated inversion recovery (FLAIR)-weighted image at onset shows hyperintense lesions in the thalamus, the mammillary bodies, and the dorsal portion of the medulla oblongata (*arrows*). **b** A photomicrograph of a labial salivary gland biopsy at the second admission. An aggregate of lymphocytes surrounding a salivary gland. Size bar is 50 μm. **c** A sagittal T2-weighted image at the fifth admission shows hyperintense lesions throughout the spinal cord (*arrowheads*). *IHMP* Intravenous high-dose methylprednisolone (1 g/day for 3 days in one course), *EDSS* expanded disability status scale

A 50-year-old female (Patient 2) visited our hospital with acute left visual loss and depression. She was diagnosed with retrobulbar optic nerve neuritis, but she rejected steroid therapy and was not admitted to our hospital. One year later, she was sent to our hospital by ambulance due to weakness. Physical examination revealed dysphagia, dysarthria, incomplete tetraplegia, urinary retention, and depression. MRI revealed T2 hyperintensities in the corpus callosum, thalamus, midbrain, and pons. She was diagnosed with CNS–SjS based on SjS criteria (Table 1), and she was treated with IHMP. Because high doses of oral steroids may exacerbate depression, we started therapy with tacrolimus (3 mg/day) to prevent relapse. No recurrence was observed for nine months, but she could not continue the therapy due to exacerbation of depression. Two years after withdrawal, she suffered right hemiplegia, and MRI revealed a relapse lesion in the left posterior limb of the internal capsule.

The serum of both patients was positive for AQP4-Ab after the initiation of tacrolimus. Because no recurrences were observed for at least 9 months for one patient (Patient 2) and 49 months for the other (Patient 1), we concluded that tacrolimus is effective in CNS–SjS with AQP4-Ab. Considering the pathological observations that indicate loss of AQP4 with deposition of antibody and compliment in CNS lesions in NMO [9, 10], we speculate that tacrolimus may act by suppressing the humoral immunity against AQP4 through Th2 inhibition.

Table 1 Clinical features of two patients

	Patient 1	Patient 2
Age at onset (years), sex	48, female	50, female
Ethnicity	Japanese	Japanese
Dry mouth	+	+
Number of relapses[a]	9	2
MRI findings		
Optic lesion	+	+
Cerebral lesion	+	+
Pontine lesion	−	+
Medullary lesion	+	−
Longitudinal cord lesion	+	−
Autoantibodies		
ANA	+	+
SS-A	+	+
SS-B	−	+
Aquaporin-4	+	+
Diagnostic tests for SjS		
Schirmer test	+	+
Saxon test	+	+
Salivary gland biopsy	Compatible for SjS	Not done
Sialography	Not done	Compatible for SjS
CSF findings		
Cells/μl	26	37
MBP (mg/dl, <4.0)	6.2	56.3
Oligoclonal IgG bands	−	−
Diagnosis		
Criteria of SjS	Fulfilled	Fulfilled
Criteria of NMO	Fulfilled	Not fulfilled

ANA antinuclear antibody, CSF cerebrospinal fluid, IgG immunoglobulin G, *MBP* myelin basic protein, MRI magnetic resonance imaging, *NMO* neuromyelitis optica, *SjS* Sjögren's syndrome

[a] Including first attack

References

1. Xue L, Gyles SL, Barrow A, Pettipher R (2007) Inhibition of PI3 K and calcineurin suppresses chemoattractant receptor-homologous molecule expressed on Th2 cells (CRTH2)-dependent responses of Th2 lymphocytes to prostaglandin D(2). Biochem Pharmacol 73:843–853. doi:10.1016/j.bcp.2006.11.021
2. Gold BG, Armistead DM, Wang MS (2005) Non-FK506-binding protein-12 neuroimmunophilin ligands increase neurite elongation and accelerate nerve regeneration. J Neurosci Res 80:56–65. doi:10.1002/jnr.20447
3. Delalande S, de Seze J, Fauchais AL, Hachulla E, Stojkovic T, Ferriby D, Dubucquoi S, Pruvo JP, Vermersch P, Hatron PY (2004) Neurologic manifestations in primary Sjögren syndrome: a study of 82 patients. Medicine (Baltimore) 83:280–291. doi:10.1097/01.md.0000141099.53742.16
4. Wingerchuk DM, Lennon VA, Lucchinetti CF, Pittock SJ, Weinshenker BG (2007) The spectrum of neuromyelitis optica. Lancet Neurol 6:805–815. doi:10.1016/S1474-4422(07)70216-8
5. Mandler RN, Ahmed W, Dencoff JE (1998) Devic's neuromyelitis optica: a prospective study of seven patients treated with prednisone and azathioprine. Neurology 51:1219–1220
6. Jacob A, Matiello M, Wingerchuk DM, Lucchinetti CF, Pittock SJ, Weinshenker BG (2007) Neuromyelitis optica: changing concepts. J Neuroimmunol 187:126–138. doi:10.1016/j.jneuroim.2007.04.009
7. Pittock SJ, Lennon VA, Seze JD, Vermersch P, Homburger HA, Wingerchuk DM, Lucchinetti CF, Zéphir H, Moder K, Weinshenker BG (2008) Neuromyelitis optica and non organ-specific autoimmunity. Arch Neurol 65:78–83. doi:10.1001/archneurol.2007.17
8. Vitali C, Bombardieri S, Jonsson R, Moutsopoulos HM, Alexander EL, Carsons SE, Daniels TE, Fox PC, Fox RI, Kassan SS, Pillemer SR, Talal N, Weisman MH (2002) Classification criteria for Sjögren's syndrome: a revised version of the European criteria proposed by the American-European Consensus Group. Ann Rheum Dis 61:554–558. doi:10.1136/ard.61.6.554
9. Misu T, Fujihara K, Nakamura M, Murakami K, Endo M, Konno H, Itoyama Y (2006) Loss of aquaporin-4 in active perivascular lesions in neuromyelitis optica: a case report. Tohoku J Exp Med 209:269–275. doi:10.1620/tjem.209.269
10. Roemer SF, Parisi JE, Lennon VA, Benarroch EE, Lassmann H, Bruck W, Mandler RN, Weinshenker BG, Pittock SJ, Wingerchuk DM, Lucchinetti CF (2007) Pattern-specific loss of aquaporin-4 immunoreactivity distinguishes neuromyelitis optica from multiple sclerosis. Brain 130:1194–1205. doi:10.1093/brain/awl371

Original Paper

European Neurology

Eur Neurol 2009;62:167–170
DOI: 10.1159/000227277

Received: June 17, 2008
Accepted: May 11, 2009
Published online: July 7, 2009

Interferon-β_{1b} Treatment in Neuromyelitis Optica

Masami Tanaka[a] Keiko Tanaka[b, c] Mika Komori[a]

[a]MS Center, Utano National Hospital, Kyoto, [b]Department of Neurology, Brain Research Institute, Niigata University, Niigata, and [c]Department of Neurology, Kanazawa Medical University, Uchinada, Japan

Key Words
Interferon · Multiple sclerosis · Neuromyelitis optica · Relapse · Anti-aquaporin-4 antibody

Abstract
Background: The effects of interferon-β_{1b} (IFN-β_{1b}) administration in multiple sclerosis (MS) patients have been confirmed, however, those in neuromyelitis optica (NMO) patients have not been shown. In this study, we assessed the effects of IFN-β_{1b} treatment on disease exacerbation and disability progression in MS or NMO patients. ***Methods:*** We reviewed a series of 104 consecutive patients with relapsing-remitting MS (RRMS) (69) or NMO (35) treated with IFN-β_{1b} in the MS clinical center of a national hospital in Japan. ***Results:*** The relapse number in the RRMS patients significantly decreased within 1 year after IFN-β_{1b} treatment ($p < 0.00001$); however, that in the NMO patients did not show a significant decrease ($p = 0.5601$). The decrease in annualized relapse rates in each RRMS patient after treatment was significant ($p < 0.01$), but that in each NMO patient was not ($p > 0.05$). The change in Kurtzke's Expanded Disability Status Scale score 1 year after treatment was higher in the NMO patients than in the RRMS patients ($p = 0.0225$). ***Conclusion:*** In NMO patients, IFN-β_{1b} treatment was not effective in reducing the relapse number and the disability progression.

Introduction

Interferon-β_{1b} (IFN-β_{1b}) treatment significantly reduces the relapse rate [1], areas of lesions, and disease activity as determined by MRI [2] in relapsing-remitting multiple sclerosis (RRMS), and delays the conversion of clinically isolated syndromes to clinically definite MS [3].

The pathogenesis of neuromyelitis optica (NMO) is predominantly antibody mediated because clinical observations show high prevalence of autoantibodies and autoimmune diseases, or high effectivity of plasmapheresis and immunosuppressive medications including azathioprine, corticosteroids, and rituximab [4]. Immunopathologic studies demonstrated the deposition of immunoglobulin and complement in spinal cord lesions. Anti-aquaporin-4 antibody (anti-AQP-4-Ab) found in the sera of patients with NMO is a disease-specific marker [5]. These findings suggest that NMO is distinct from MS, although the effector cells causing demyelinating lesions in the central nervous system and encephalitogenic antigens reacting with effector cells in MS have not yet been identified. Most neurologists in Western countries consider that IFN-β is ineffective for NMO patients [4]. A recent study has shown that the relapse-free period is shorter in 7 NMO patients treated with IFN-β than in 19 NMO patients treated with immunosuppressive drugs [6]; however, the number of patients observed was very

KARGER
Fax +41 61 306 12 34
E-Mail karger@karger.ch
www.karger.com

0014–3022/09/0623–0167$26.00/0

Accessible online at:
www.karger.com/ene

Dr. M. Tanaka
8 Ondoyama, Narutaki, Ukyo-ku
Kyoto 616-8255 (Japan)
Tel. +81 75 461 5121, Fax +81 75 464 0027
E-Mail tanaka@unh.hosp.go.jp

small. We reviewed the medical records of our Japanese patients with NMO and determined whether IFN-β_{1b} treatment affects disease exacerbation and disability progression as indicated by an increase in Kurtzke's Expanded Disability Status Scale (EDSS) score [7] in patients with NMO.

Methods

We conducted a retrospective study by examining the medical records of 104 consecutive patients treated with IFN-β_{1b} at one national center from December 2000 to December 2005, including 69 patients with RRMS (19 men, 50 women), aged 16–69 years, who fulfilled McDonald's criteria [8], and 35 patients with relapsing NMO (3 men, 32 women), aged 28–78 years, who fulfilled the criteria proposed by Wingerchuk et al. [9]. The NMO patients in this study did not show systemic autoimmune diseases. The durations from onset were 3–46 years in the RRMS patients and 3–35 years in the NMO patients. The patients received 250 μg of IFN-β_{1b} (Betaferon) subcutaneously every other day for 1 year. Of the 35 patients with NMO, 19 showed anti-AQP-4-Ab in their sera.

Patients with primary or secondary progressive MS and relapsing optic neuritis were excluded from the study. We did not include spinal MS patients because transition to classic MS or NMO from spinal MS is common in patients with short disease duration such as 5 years. We did not include in this study the patients whose IFN-β_{1b} treatment was stopped because of the development of skin ulcers (3 RRMS patients and 3 NMO patients, 1 of them was positive for anti-AQP-4-Ab), liver dysfunction (2 RRMS patients), relapsing pneumonia (1 NMO patient negative for anti-AQP-4-Ab), fever, and depression (1 RRMS patient each) within 1 year of IFN-β_{1b} treatment. We excluded 2 patients who were started on IFN-β_{1b} treatment together with mitoxantrone or steroid pulse therapy every 3 months (1 RRMS patient each). One RRMS patient was excluded from this study because of irregular IFN-β_{1b} treatment.

Relapse was defined as the appearance of a new symptom or the worsening of an old symptom caused by MS, accompanied by a documented new neurological abnormality lasting for at least 48 h and preceded by a stable condition or improvement for at least 30 days. We compared the decrease in relapse number (expressed as relapse number within 1 year after IFN-β_{1b} treatment minus that within 1 year before IFN-β_{1b} treatment) of the RRMS patients with that of the NMO patients.

Kurtzke's EDSS score [7] was used to evaluate the clinical ratings. We compared the EDSS score of each patient at the start of treatment and 1 year after treatment and compared the change in the EDSS score of each patient expressed as the score after treatment minus the score before treatment.

The statistical significance of the difference in values was determined by Fisher's exact test for the change in the percentage of patients showing relapse, by Mann-Whitney U test for the decrease in relapse number and for the change in the EDSS score after treatment with IFN-β_{1b}, by Wilcoxon's signed-rank test for the change in annualized relapse rates in each patient before and after treatment, and by McNemar's test for the change in the relapse number or EDSS scores before and after treatment.

Anti-AQP-4-Ab in the serum samples was examined by an indirect immunofluorescence method reported previously [10] using HEK-293 cells transfected with an AQP-4 expression vector containing a full-length cDNA of human AQP-4. The examiner (K.T.) of the anti-AQP-4-Ab was blind to all the clinical information including the clinical phenotype of the patients.

This study was approved by the Medical Ethics Committee of Utano National Hospital. All the participants provided their written informed consent.

Results

Of the 69 (75.4%) RRMS patients, 52 showed relapse before treatment but only 24 (34.8%) showed exacerbation after IFN-β_{1b} treatment. Of the 35 patients with NMO, 26 (74.3%) showed exacerbation before treatment and 25 (71.4%) showed exacerbation after treatment. The change in the percent of patients showing exacerbation before and after treatment was not different between the RRMS and NMO patients as determined by Fisher's exact test ($p = 0.0629$); however, the relapse number in the RRMS patients significantly decreased 1 year after treatment (from 97 to 39; $p < 0.00001$) as determined by McNemar's test; on the other hand, that in the NMO patients did not show a significant decrease (from 76 to 72; $p = 0.5601$) as determined by McNemar's test (table 1).

The decrease in relapse number after treatment with IFN-β_{1b} was higher in the RRMS patients (from –2 to 5; 0.74 ± 1.31) than in the NMO patients (from –3 to 3; 0 ± 1.60) as determined by Mann-Whitney test ($p = 0.0375$). The annualized relapse rates in each RRMS patient after treatment (0–4) were significant ($p < 0.01$), but those in each NMO patient (0–6) were not as determined by Wilcoxon's signed-rank test ($p > 0.05$). In the patients with NMO, the decrease in exacerbation number after treatment with IFN-β_{1b} was not significantly different between the anti-AQP-4-Ab-positive group (from –3 to 2 in 19 patients) and the anti-AQP-4-Ab-negative group (from –3 to 3 in 16 patients) as determined by Mann-Whitney test ($p = 0.3696$). The decreases in the annualized relapse rates after treatment in each NMO patient with anti-AQP-4-Ab ($p > 0.05$) and in each NMO patient without anti-AQP-4-Ab were not significant as determined by Wilcoxon's signed-rank test ($p > 0.05$).

The EDSS scores of the patients with RRMS and NMO before treatment with IFN-β_{1b} were 3.85 ± 2.47 (mean ± SD; from 0 to 7.5) and 5.02 ± 2.27 (from 0 to 8.5), and those after the treatment were 4.10 ± 2.63 (from 0 to 7.5) and 5.61 ± 2.76 (from 0 to 9), respectively. The EDSS score of the NMO patients was higher than that of the

Table 1. Effects of IFN-β_{1b} treatment on exacerbation number in patients with MS and NMO

	MS (n = 69)		NMO (n = 35)		p
	before Tx[1]	after Tx	before Tx	after Tx	
Percentage of patients showing relapses	75.4%	34.8%	74.3%	71.4%	0.0629[2]
Total exacerbation number	97	39	76	72	
	$p < 0.00001$[3]		$p = 0.5601$[3]		
Annualized relapse rate, mean (range)	1.28 (0–4)	0.58 (0–4)	2.05 (0–6)	1.85 (0–6)	
	$p < 0.001$[4]		$p > 0.05$[4]		

The exacerbation number was determined during the periods 1 year before and after IFN-β_{1b} treatment. MS = Multiple sclerosis; NMO = neuromyelitis optica.

[1] Tx: treatment with IFN-β_{1b}. [2] Determined by Fisher's exact test. [3] Determined by McNemar's test. [4] Determined by Wilcoxon's signed-rank test. [5] Determined by Mann-Whitney test.

Table 2. Comparison of disease progression represented by increase in EDSS score after treatment with IFN-β_{1b} between patients with MS and NMO

	MS (n = 40)		NMO (n = 26)		p
	baseline	after Tx	baseline	after Tx	
EDSS score	3.85 ± 2.47	4.10 ± 2.63	5.02 ± 2.27	5.61 ± 2.76	
	$p < 0.0008$[1]		$p < 0.0001$[1]		
Change in EDSS score after Tx	−2 to 2.5		0–3.5		
	0.31 ± 0.72		0.92 ± 1.08		0.0225[2]

The EDSS score was determined at the start of treatment (baseline) and 1 year after treatment. MS = Multiple sclerosis; NMO = neuromyelitis optica.

[1] Determined by McNemar's test. [2] Determined by Wilcoxon's signed-rank test.

RRMS patients before the treatment as determined by Mann-Whitney test ($p = 0.0318$). Both patient groups showed increased EDSS scores after the treatment; however, the NMO patients showed more pronounced worsening ($p < 0.0001$) than the RRMS patients ($p < 0.0008$) as determined by McNemar's test. We directly compared the change in the EDSS score between the RRMS patients and the NMO patients. The change in the EDSS score, obtained as the EDSS score after treatment minus the EDSS score at the start of treatment, was higher in the NMO patients (0.92 ± 1.08; from 0 to 3.5) than in the RRMS patients (0.31 ± 0.72; from −2 to 2.5) as determined by Mann-Whitney test ($p = 0.0225$) (table 2). In the patients with NMO, the change in the EDSS score was not significantly different between the anti-AQP-4-Ab-positive group (from 0 to 3.5 in 12 patients) and the anti-AQP-4-Ab-negative group (from 0 to 2.5 in 9 patients) as determined by Mann-Whitney test ($p = 0.6511$).

Discussion

We examined the effect of IFN-β_{1b} treatment on the exacerbation number during the periods 1 year before and after treatment, and on the change in the EDSS score at the start of treatment and 1 year after treatment in the patients with RRMS and NMO. This study showed that IFN-β_{1b} treatment can suppress relapses in the RRMS patients as reported in European and North American populations [11], but cannot inhibit the increase in the EDSS score. In the patients with NMO, treatment with IFN-β_{1b} did not significantly suppress the relapse numbers or the increase in EDSS score (tables 1 and 2, respectively). To compare the effect of IFN-β_{1b} treatment on the change in the EDSS score of the patients with RRMS and NMO, we reviewed the difference in the EDSS scores at the start of IFN-β_{1b} treatment and 1 year after the treatment in both patient groups. The increase in the EDSS score was high-